Title
INJECTION AND ENERGY RECOVERY IN FRACTURED GEOTHERMAL RESERVOIRS

Authors
Bodvarsson, G.S.
Pruess, K.
O'Sullivan, M.J.

Publication Date
1983

LBL-15344

Lawrence Berkeley Laboratory
UNIVERSITY OF CALIFORNIA

EARTH SCIENCES DIVISION

To be presented at the Society of Petroleum Engineers, 53rd Annual California Regional Meeting, Ventura, CA, March 23-25, 1983

INJECTION AND ENERGY RECOVERY IN FRACTURED GEOTHERMAL RESERVOIRS

Gudmundur S. Bodvarsson, Karsten Pruess, and Michael J. O'Sullivan

January 1983

Prepared for the U.S. Department of Energy under Contract DE-AC03-76SF00098

LBL-15344

DISCLAIMER

To be presented at Society of Petroleum Engineers 53rd Annual California Regional Meeting, March 23-25, 1983, Ventura, Ca.

LBL 15344

INJECTION AND ENERGY RECOVERY IN FRACTURED GEOTHERMAL RESERVOIRS

Gudmundur S. Bodvarsson and Karsten Pruess
Lawrence Berkeley Laboratory
University of California
Berkeley, California 94720

Michael J. O'Sullivan
University of Auckland
Auckland, New Zealand

ABSTRACT

Numerical studies of the effects of injection on the behavior of production wells completed in fractured two-phase geothermal reservoirs are presented. In these studies the multiple-interacting-continua (MINC) method is employed for the modeling of idealized fractured reservoirs. Simulations are carried out for a five-spot well pattern with various well spacings, fracture spacings, and injection fractions. The production rates from the wells are calculated using a deliverability model. The results of the studies show that injection into two-phase fractured reservoirs increases flow rates and decreases enthalpies of producing wells. These two effects offset each other so that injection tends to have small effects on the usable energy output of production wells in the short term. However, if a sufficiently large fraction of the produced fluids is injected, the fracture system may become liquid-filled and an increased steam rate is obtained. Our studies show that injection greatly increases the long-term energy output from wells, as it helps extract heat from the reservoir rocks. If a high fraction of the produced fluids is injected, the ultimate energy recovery will increase manyfold.

INTRODUCTION

At present reinjection of geothermal brines is employed or being considered at most high-temperature geothermal fields under development. At many geothermal fields, primarily those in the U.S. or Japan, reinjection is a necessity because environmental considerations do not permit surface disposal of the brines (unacceptable concentrations of toxic minerals). At other fields, e.g., The Geysers, California, reinjection is used for reservoir management to help maintain reservoir pressures and to enhance energy recovery from the reservoir rocks. The effectiveness of injection in maintaining reservoir pressures has been illustrated at the Ahuachapán geothermal field in El Salvador (Cuellar, 1981).

During the last decade various investigators have studied the effects of injection on pressures and overall energy recovery from geothermal fields. Theoretical studies have been carried out by Kasameyer and Schroeder (1975), Lippmann et al. (1977), O'Sullivan and Pruess (1980), Schroeder et al. (1982), and Pruess (1983a), among others. Site-specific studies were reported by Morris and Campbell (1979) on East Mesa, California; Schroeder et al. (1982) and Giovannoni et al. (1981) on Larderello, Italy; Bodvarsson et al. (1983) on Baca, New Mexico; Tsang et al. (1982) on Cerro Prieto, Mexico; and Jonsson (1979) and Pruess et al. (1983) on Krafla, Iceland. These studies have given valuable insights into physical processes and reservoir response during injection. However, there is limited understanding of injection effects in fractured reservoirs, especially high-temperature two-phase systems. Fundamental studies and quantitative results for the design of injection programs in such systems are greatly needed.

The objectives of the present work are to investigate the effects of injection on the behavior of fractured two-phase reservoirs. Some of the questions to be addressed are:

(1) How will injection affect flow rates and enthalpies of the production wells?
(2) Can injection increase the short-term usable energy output of wells?
(3) What are the long-term effects of injection?
(4) How is the efficiency of injection dependent on factors such as well spacing and fracture spacing?

Reliable answers to these questions should be valuable for field operators in the design of injection systems for two-phase fractured reservoirs.

APPROACH

In the present work we consider wells arranged in a five-spot pattern (Figure 1). Due to symmetry we only need to model 1/8 of a basic element as shown in Figure 1; however, our results are always presented for the full five-spot. The "primary" (porous medium) mesh shown in Figure 1 consists of 38 elements; some of the smaller ones close to the wells are not shown. The mesh has a single layer, so that gravity effects are neglected. The fractured reservoir calculations are carried out by means of the "multiple interacting continua" method (MINC; Pruess and Narasimhan, 1982), which is a generalization of the double-porosity concept introduced by Barenblatt et al. (1960) and Warren

References and illustrations at end of paper.

and Root (1963). The basic reservoir model consists of rectangular matrix blocks bounded by three sets of orthogonal infinite fractures of equal aperture b and spacing D (Figure 2a). In the mathematical formulation the fractures with high transport and low storage capacity are combined into one continuum and the low permeability, high storativity matrix blocks into another. The MINC method treats transient flow of fluid (steam and/or water) and heat between the two continua by means of numerical methods. Resolution of the pressure and temperature gradients at the matrix/fracture interface is achieved by partitioning of the matrix blocks into a series of interacting continua. These are defined on the basis of distance from the nearest fracture, giving rise to a set of nested volume elements, as shown schematically in Figure 2b. A partitioning procedure analogous to the idealization in Figure 2b can be carried out for each of the grid blocks of the "primary" five-spot mesh, resulting in a "secondary" mesh which includes global ("interblock") flow through the fracture network, while matrix and fractures can exchange fluid and heat locally within the grid blocks of the primary mesh ("intrablock flow"). Quantitative details on the mesh construction are given in Pruess and Narasimhan (1982). The MINC method has been validated against a number of analytical solutions (Pruess and Narasimhan, 1982; Lai, Bodvarsson, and Pruess, 1983). The present work employs a schematic reservoir model with regularly shaped matrix blocks (see Figure 2), but realistic irregular fracture distributions can also be handled with the MINC method (Pruess and Karasaki, 1982).

The injection and production wells are assumed to be open only to the fracture system. The production wells are modeled using a deliverability model that allows flow rates to decline realistically with time as the reservoir is depleted. The flow rate q produced from a well completed in a two-phase reservoir is calculated from:

$$q = PI \times \left[\frac{k_\ell \rho_\ell}{\mu_\ell} + \frac{k_v \rho_v}{\mu_v}\right](P - P_{wb}) \qquad (1)$$

where P is the pressure of the two-phase fluid in the grid block containing the well, P_{wb} is the flowing bottomhole pressure, and PI is the productivity index. Other symbols are defined in the Nomenclature. The flowing enthalpy, h, is given by:

$$h = \frac{\frac{k_\ell \rho_\ell}{\mu_\ell} h_\ell + \frac{k_v \rho_v}{\mu_v} h_v}{\frac{k_\ell \rho_\ell}{\mu_\ell} + \frac{k_v \rho_v}{\mu_v}} \qquad (2)$$

where h_ℓ and h_v are the saturated enthalpies of liquid and vapor at reservoir conditions, respectively.

The injection rate q_i is taken to be a prescribed fraction f of the production rate

$$q_i = f \cdot q. \qquad (3a)$$

The parameter f, which expresses the ratio of injection rate to production rate, will be referred to as "injection fraction" or "injection factor." In the numerical simulation we use the approximation

$$q_i^{k+1} = f \cdot q^k, \qquad (3b)$$

i.e., the injection rate during time step k+1 is specified as a fraction of the production rate for the previous time step. This approximation introduces negligible inaccuracy, while giving a substantial improvement in calculational efficiency over the more rigorous prescription $q_i^{k+1} = f \cdot q^{k+1}$.

The calculations were carried out with LBL's general-purpose simulator MULKOM (Pruess, 1983b). In its geothermal mode, MULKOM is similar to SHAFT79, against which it has been thoroughly validated (Pruess and Schroeder, 1980; Pruess, 1983a). The reservoir fluid is assumed to be pure water substance. The thermophysical properties are represented by the steam-table equations, as given by the International Formulation Committee (1967).

The enthalpy of produced fluids generally changes with time, which will affect wellbore pressure drop and bottomhole pressure, and in turn the flow rate (Equation 1). In the simulations these effects are neglected, and a constant flowing bottomhole pressure, P_{wb}, is assumed. For a more rigorous calculation of the flowrate one must employ a wellbore model. However, this causes further computational difficulties as well as introducing the arbitrary choice of parameters such as depth to the producing interval, casing structure, slotted interval, well diameters, friction factors, etc. In many cases the wellbore effects may not be significant. Otherwise a wellbore model should be used with the appropriate site-specific parameters.

MODEL PARAMETERS

Values chosen for the well and reservoir parameters correspond to low-permeability two-phase fractured reservoirs such as those at Baca, New Mexico; Krafla, Iceland; and Olkaria, Kenya. Table 1 gives values for fixed parameters; values for those parameters that were varied are given in Table 2. Values for the thermal and hydraulic parameters of the rock matrix (given in Table 1) are typical for fractured volcanic rocks. The fracture porosity was chosen as 0.01 on the basis of a recent report by Weber and Bakker (1981). The linear relative permeability curves used gave reasonable results in the modeling of the natural state of the Krafla geothermal field in Iceland (Bodvarsson et al., 1982). Similarly, the values chosen for the productivity index (PI) and the bottomhole pressure (P_{wb}) are typical for Krafla wells (Pruess et al., 1983).

In the present work we studied injection effects in dependence upon well and fracture spacing, initial vapor saturation, and injection fraction. The values used for these parameters are given in Table 2.

RESULTS

Using the parameter values given in Tables 1 and 2, a series of simulations were carried out. In most cases the reservoir system was simulated for a time of 15 years, which is sufficient for investigating shorter-term effects of injection. In a few cases the simulations were carried out for much longer times in order to study the long-term effects of injection on the thermal and hydrologic depletion of a fractured

reservoir. In the following discussion the short- and long-term effects of injection will be considered in separate sections.

The simulations generated large amounts of data on production rates and enthalpies, injection pressures, thermal sweep, reservoir depletion, migration of thermal and hydraulic fronts in fractures and matrix, etc. In the present work we are primarily interested in the effects of injection on the behavior of the production wells, especially the usable steam rate produced. The usable steam rate at the separators is given by the following expression:

$$q_v^s = q \times \frac{h - h_\ell^s}{h_v^s - h_\ell^s} \qquad (4)$$

where h_ℓ^s and h_v^s are the saturated liquid and vapor enthalpies, respectively, at separator conditions. Equation (4) approximates the two-phase flow from the wellbottom to the separators as an iso-enthalpic expansion. In the present work we use a separator pressure of 9 bars. As the enthalpy of saturated steam does not vary much with pressure, a different separator pressure will not significantly alter the results.

SHORT-TERM EFFECTS OF INJECTION

First, let us consider the case of large production well spacing (1000 m), large fracture spacing (250 m), and an initial vapor saturation of 10%. Figures 3-5 show the production rate, enthalpy, and steam rate at the separators (hereafter referred to as steam rate) as a function of time, respectively. Figures 3 and 4 show that in the no-injection case the flow rate declines and the enthalpy increases monotonically with time as is to be expected. The enthalpy does not reach a stable value as in the case of an infinite reservoir system (O'Sullivan, 1981) because of the bounded drainage area. Figures 3 and 4 also show that injection has large effects on the flow rates and enthalpies of the production wells, even for the large well spacing (1000 m) in this case. The flow rates increase markedly in response to injection and much more so for the 100% injection case than the 50% one. After 15 years of production the flow rate is 32 and 83% higher than in the no-injection case, for injection fractions of 0.5 and 1.0, respectively. However, injection also causes an enthalpy decline (Figure 4) and after 15 years the enthalpy is 11 and 20% lower than in the no-injection case for injection fractions of 0.5 and 1.0, respectively.

In order to determine the net effect of flow rate increase and enthalpy decline on the usable thermal power output of the production well, one must consider the steam rate obtained after flashing at the separators. Figure 5 shows that there is little difference in steam rate between the injection cases and the no-injection case at all times. The differences, however, gradually increase with time, suggesting that in the long run, injection may significantly increase the energy output of the well. In the short run the benefits of the large flow rate increases due to injection are almost entirely offset by the accompanying decline in enthalpy of the produced fluids. It should be emphasized that, if the effects of enthalpy changes on the bottomhole pressure are taken into account, the slight differences in steam rates will decrease even further.

It can be shown analytically that, as long as production wells remain in two-phase conditions, there is a general tendency for flow rate and enthalpy effects of injection to compensate each other, yielding remarkably small net change in usable steam rate produced. Substituting Equations (1) and (2) into (4), the steam rate at the separators can be written:

$$q_v^s = \frac{PI(P - P_{wb})}{h_v^s - h_\ell^s}\left[k_\ell \frac{\rho_\ell}{\mu_\ell}(h_\ell - h_\ell^s) + k_v \frac{\rho_v}{\mu_v}(h_v - h_\ell^s)\right] \qquad (5)$$

Equation (5) shows that for given well and separator conditions, the steam rate depends primarily upon (i) reservoir pressure P, and (ii) relative permeabilities k_ℓ and k_v (or liquid and steam mobilities). In two-phase systems, pressures are controlled by temperatures, which tend to change slowly with time due to the large heat capacity of the reservoir rocks. Our simulations have shown that injection has little effect on temperatures and pressures in reservoir regions which remain in two-phase condition. Injection does increase pressures in the flooded (single-phase) regions, but production wells tend to remain in two-phase or slightly subcooled liquid conditions in most cases, even when injection fraction approaches 100%. Therefore, pressure effects from injection tend to be small near production wells. Changes in production rates as a consequence of injection are almost entirely due to mobility effects, i.e., variations in relative permeabilities to vapor and liquid in dependence upon vapor saturation.

Mobility effects are represented by the terms in square brackets in Equation (5). To analyze these effects we have investigated the dependence of the steam rate on vapor saturation for different relative permeability curves. We selected the relative permeability curves shown in Figure 6, as these are the curves most frequently employed in the numerical simulation of geothermal reservoirs. Furthermore, we use the well and separator parameters given in Table 1 and a reservoir temperature of 300°C (P_{sat} = 85.9 bars).

Figure 7 shows the steam rate at the separators versus vapor saturation for the different relative permeability curves. The figure shows that for curves which have the characteristic that $k_\ell + k_v = 1$ for all saturations (x-curves and Grant's (1977) curves), the steam rate at the separators is practically independent of the vapor saturation. The reason for this is that

$$\frac{\rho_\ell}{\mu_\ell}(h_\ell - h_\ell^s) \approx \frac{\rho_v}{\mu_v}(h_v - h_\ell^s) \qquad (6)$$

for most practical values of reservoir temperature (200-325°C) and separator pressure (5-9 bars), so that the term in square brackets in Equation (5) is approximately given by $(k_\ell + k_v)(\rho_\ell/\mu_\ell)(h_\ell - h_\ell^s)$. In the case of the linear relative permeability curves (the ones used in the injection simulations) there is a rather weak dependence of the steam rate on vapor saturations, because $k_\ell + k_v \lesssim 1$ for $0 < S < 1$. At lower vapor saturations the steam rate increases slightly with decreasing vapor saturation, which is the reason that the steam rate is slightly higher in the injection cases than in the no-injection case discussed above. Note that for the linear relative permeability curves the steam rate increases with increasing vapor saturation when the liquid phase is immobile ($S > 0.7$).

This will have some implication in simulations discussed in later sections. Figure 7 shows that for the Corey curves the steam rate is strongly dependent upon the vapor saturation, giving rise to favorable effects of injection on the short-term steam rates. However, there is growing evidence that the Corey curves are not applicable to fractured geothermal reservoirs (see for example Bodvarsson et al., 1982).

Plots of flow rate (Equation (1)) and flowing enthalpy (Equation (2)) versus vapor saturation show that the flow rate will increase drastically and the enthalpy will decrease with decreasing vapor saturation for all of the relative-permeability curves. One can therefore safely conclude from these analytic considerations that the flow rate increases and enthalpy declines exhibited in the simulations are simply mobility (relative permeability) effects. Figure 7 shows that impacts on usable power output from injection can be expected to be small, as long as the fracture system around the production well remains in two-phase conditions.

EFFECTS OF WELL SPACING

Figures 8-10 show the results of a series of simulations with the same parameters as before, but a smaller production well spacing (250 m). In this case, the production rate is at all times smaller and the enthalpy rise more rapid for no-injection than in the case of larger well spacing. Superheated steam is produced after only 4 years of production. This is a result of the small drainage area and the associated boundary effects. Figures 8 and 9 also show that the mobility effects (rise in flow rate and decline of enthalpy) due to injection are much stronger for the 100%-injection case than for the 50%-injection case.

When 50% of the produced fluids are injected, the enthalpy rises gradually, but two-phase fluids are produced at all times. The flow rates are only slightly higher than those in the no-injection case. In the 100%-injection case, the flow rates are only weakly dependent on the well spacing; the flow rate increases at early times due to mobility effects, but after the injected fluid has flooded the fracture system, a quasi-steady state flow field develops with a near-constant production rate of 20 kg/s. The slight decrease at later times is due to the decline in fluid temperature and increase in viscosity.

The enthalpy of the produced fluids in the 100%-injection case reflects thermal interference of the colder injected fluids as the enthalpy declines below the saturated liquid enthalpy at reservoir conditions (h_ℓ = 1340 kJ/kg at T = 300°C) after only 3 years. The enthalpy decline continues thereafter as more colder fluids migrate to the production well. The early breakthrough of the injected water at the production well is caused by a combination of the small well spacing (the distance from the injection well to the producer is only $250/\sqrt{2} \simeq 177$ m), the high flow rates, and the large fracture spacing. For large fracture spacing, there is a relatively small surface area between the fractures and the rock matrix, and consequently heat flow to the colder injected water is limited (Bodvarsson and Tsang, 1982). The Kakkonda geothermal field in Japan has shown thermal interference in production wells that are located less than 200 m from the injector (Horne, 1981). Simulation studies for this case have predicted thermal interference in agreement with the field observations (Witherspoon et al., 1982).

In spite of the large decline in enthalpy due to thermal interference, the 100%-injection gives considerably higher steam rate at the separator than the no-injection case (50% higher after 15 years; Figure 10). The reason for these beneficial shorter-term effects of injection is that the fracture system was flooded by the injected fluid, and single-phase liquid conditions developed everywhere, causing increases in reservoir pressure near the producers. Note that in the 50%-injection case the fractures feeding the production well remain in two-phase conditions during the simulation (Figure 9) and consequently there is little or no gain in the net usable energy. The peak in the flow rate and steam rate curves in the no-injection case after 9.5 years is due to the relative permeability curves used (in the linear curves the steam mobility increases as $S \to 1$ after the liquid phase has become immobile, see Figure 6).

EFFECTS OF FRACTURE SPACING

In all of the simulations we use the same average fracture permeability to allow direct comparison between all cases. The fracture spacing affects the surface area between the rock matrix and the fractures, with smaller fracture spacing yielding larger fluid and heat transfer between matrix and fractures. In the case of no-injection, a decreased fracture spacing gives rise to higher recharge of fluids from the rock matrix into the fracture system, so that the boiling zone around the production well is less localized. This in turn results in higher flow rates and lower enthalpies at any given time. In Figure 11 the steam rate at the separator is shown for the case of 250 m production well spacing and fracture spacings of 10 and 250 m. To avoid overcrowding the figure, we omit the results for the 50%-injection case. The figure shows that in the case of no-injection the steam rate is at most times considerably higher for the small fracture spacing. This is a consequence of the higher recharge rate from the rock matrix when the fracture spacing is smaller. At late times (12-15 years), however, the steam rate drops drastically in the case of 10 m fracture spacing, as the entire reservoir system has dried up to single-phase steam conditions, and reservoir pressures fall rapidly. In the case of the larger fracture spacing, the flow rates are lower so that single-phase vapor conditions are not reached within the 15-year simulation time. The kinks in the curves in the no-injection cases are again due to the peculiar characteristics of the relative permeability curves used.

Fracture spacing affects injection response in several ways. For smaller fracture spacing, the matrix/fracture interface area is enhanced, so that more injected fluid is lost from the fractures to the rock matrix, while more matrix fluid can be tapped at the production wells. The matrix/fracture heat transfer area is of crucial importance, especially for small spacing between producers and injectors. Figure 11 shows that enhancement of energy recovery for 100% injection is more pronounced when fracture spacing is small. The steam rate for the small fracture spacing and 100% injection remains practically constant at approximately 6 kg/s over 15 years, whereas the steam rate drops rapidly for the case with the larger fracture spacing. This is a result of the thermal breakthrough of the injected water into the production well in the case of 250 m fracture spacing and the associated continual decline in enthalpy (see Figure 9). In contrast, in the case of 10 m fracture

spacing, produced enthalpy initially falls rapidly to the liquid enthalpy at reservoir conditions (about 1340 kJ/kg), and is subsequently maintained at this value due to efficient heat conduction from the matrix.

EFFECTS OF INITIAL VAPOR SATURATION

In addition to the series of simulations using an initial vapor saturation of 0.1, several cases were simulated with an initial vapor saturation of 0.3. The results showed the same general trends as we have discussed for 10% initial vapor saturation. In the cases without injection, flow rates were generally lower and the enthalpies of the produced fluids higher at all times. The smaller initial fluid mass in the reservoir also caused a more rapid reservoir depletion.

The mobility effects due to injection were stronger for the cases with higher initial vapor saturation, as is to be expected. However, the effects of injection on the steam rate at the separators were generally weaker since it took longer for the injected water to flood the fracture system.

LONG-TERM EFFECTS OF INJECTION

It is of interest to investigate the long-term effects of injection, and especially how injection affects the ultimate energy recovery from the reservoir system. Several of the cases shown in Table 2 were simulated until the energy output of the production well became negligibly small, as the reservoir system was depleted thermally or hydrologically. In the following discussion we will consider the case of 250 m well spacing, 250 m fracture spacing, and an initial vapor saturation of 10%. This case was selected as it represents rather unfavorable conditions for injection, with thermal breakthrough experienced after only 3 years of production/injection. In cases of larger well spacing and smaller fracture spacing, the long-term effects of injection will be far more favorable than in the present case.

The trends of flow rate decline shown in Figure 8 continued after 15 years, with the production rate becoming negligibly small after 50 and 150 years for the no-injection and 50%-injection cases, respectively. The flow rate in the 100%-injection case continued to decline gradually due to the enthalpy decline, but reached a steady-state value of 29.6 kg/s after 80 years of simulation. The enthalpy in the 100%-injection case declined monotonically towards the enthalpy of the injected water (632 kJ/kg). The enthalpy of the produced fluids in the 50%-injection case increased monotonically, with saturated steam produced after 80 years of simulation.

The steam rate at the separators is shown in Figure 12 for the three cases. The steam rate declines rapidly in the no-injection and 50%-injection cases as the reservoir approaches fluid depletion. The more gradual decline of the steam rate in the 100%-injection case is caused by the slower thermal depletion (enthalpy decline). The enthalpy in the 100%-injection case approaches that of liquid water at separator conditions after 220 years of simulation.

The total original heat in place in the reservoir is 2.48×10^{16} W·s per production well, relative to the injection temperature of 150°C. Of this heat, fractions of 29.2%, 44.8%, and 96.0% were recovered as usable thermal energy (steam at separator conditions) for the cases with injection factors of 0, 50, and 100%, respectively. This result clearly demonstrates the potentially large long-term benefits of full reinjection. At the end of the simulations, the reservoir has an average temperature of 280 and 258°C for the no-injection and 50%-injection cases, respectively. In these fluid-limited cases there is a vast amount of energy remaining, but the reservoir pressure has declined to 20 bars at the production well, with production rate approaching zero. On the other hand, at the end of the 100%-injection simulation, the reservoir pressure and production rate are still high, but the temperature has declined to that of the injected water (150°C) in most of the reservoir, with separator temperature (T_s = 175.4°C at p_s = 9 bars) reached near the production well. The cumulative net energy output of the production well is plotted versus time for the three cases in Figure 13. The steam rate was converted to electric power using a realistic conversion factor of 2.2 kg/MW·s. The figure shows that the total electric energy output of the well is 38, 58, and 125 MW·years, for injection fractions of 0, 50%, and 100%, respectively.

FIELD EXAMPLE

Injection test data that verify some of the analysis presented in this paper have been reported by Armannsson et al. (1982) and Stefansson et al. (1982). The data are from two wells at the Krafla geothermal field (wells 7 and 13). The wells are approximately 200 m apart and both are completed in the lower two-phase reservoir (well 7 is also open in the upper liquid reservoir; Stefansson, 1981). Both wells have scaling problems that require periodical cleaning; during the cleaning operation cold water is injected into the wells. Figure 14 shows the response of well 13 to the cold-water injection into well 7. In late August 1980, well 13 was producing approximately 6 kg/s of almost pure steam (enthalpy of 2660 kJ/kg). The injection into well 7 started in early September and on September 5 an increase in the water production was noticed (Stefansson et al., 1982). Repeated flow tests were conducted after that until the well was connected to the steam lines. The flow rate, enthalpy, and steam rate behavior shown in Figure 14 displays features which agree very well with the theoretical studies presented above. The mobility effects due to injection cause large increases in the flow rate and decreases in enthalpy, but the steam rate remains practically unchanged. This indicates that the sum of liquid and vapor relative permeabilities changes little with vapor saturation in this case, i.e., $k_\ell + k_v \approx 1$. Similar behavior has also been observed in well 7 when well 13 was cleaned. As other wells at Krafla are not affected, it is probable that wells 7 and 13 intersect the same fracture or fracture system (Stefansson et al., 1982).

CONCLUSIONS

The primary conclusions of our studies of injection into fractured two-phase reservoirs are:

1. Injection tends to reduce vapor saturations in the fracture system by flooding of fractures and steam condensation. This in turn increases the mobility of the fluids, which results in increased flow rates and decreasing enthalpies at the production wells. The short-term enthalpy decline is not due to thermal breakthrough of the colder injected water.

2. If the production wells remain in two-phase conditions, injection will generally have small effects on usable heat output in the short run.

3. If the injected water floods the entire fracture system so that single-phase liquid is produced, the usable thermal power output (flashed steam rate at the separators) can increase by 50% or more.

4. Injection effects increase strongly when an increased fraction of the produced fluids is injected.

5. In the long run, injection can increase the usable energy output of wells manyfold, as it helps to extract energy from the reservoir rocks, and to maintain high flow rates.

6. Field data from wells at the Krafla geothermal field in Iceland verify some of the results obtained in this study.

NOMENCLATURE

f	injection fraction (fraction of production rate injected)
h	flowing enthalpy (kJ/kg)
h_β	specific enthalpy of β phase (kJ/kg)
h_β^s	specific enthalpy of β phase at separator conditions (kJ/kg)
k	timestep counter
k_β	relative permeability of β phase
P	reservoir pressure (pascals)
PI	productivity Index (m^3)
P_s	separator pressure (pascals)
P_{sat}	saturation pressure (pascals)
P_{wb}	bottomhole pressure (pascals)
q	production rate (kg/s)
q_i	injection rate (kg/s)
q_v^s	steam rate at separators (kg/s)
S	vapor saturation (dimensionless)
$S_{\ell r}$	irreducible liquid saturation (dimensionless)
S_{sr}	irreducible steam saturation (dimensionless)
T_s	separator temperature (°C)
β	phase ($\beta = \ell$: liquid; $\beta = v$: vapor)
μ_β	viscosity of β-phase (kg/m·s)
ρ_β	density of β-phase (kg/m^3)

ACKNOWLEDGMENT

The authors are indebted to Paul Witherspoon for his continued interest and encouragement in the course of this work. We thank Drs. M. Lippmann and J. Wang for a critical review of the manuscript and valuable suggestions. The help of Peter Fuller with the numerical calculations is gratefully appreciated.

This work was supported by the Assistant Secretary for Conservation and Renewable Energy, Office of Renewable Energy, Division of Geothermal Energy and Hydropower Technologies of the U. S. Department of Energy under Contract No. DE-AC03-76SF00098.

REFERENCES

Armannsson, H., Sigurdsson, K. H., and G. Gislason, Various internal reports on flow test data from Krafla wells, Orkustofnun, National Energy Authority of Iceland, 1982.

Barenblatt, G. E., Zheltov, I. P., Kochina, I. N., "Basic Concepts in the Theory of Homogeneous Liquids in Fissured Rocks," Journal Applied Mathematics (USSR), 24(5), pp. 1286-1303 (1960).

Bodvarsson, G. S., and Tsang, C. F., "Injection and Thermal Breakthrough in Fractured Geothermal Reservoirs," Journal of Geophysical Research, vol. 87, no. B2, p. 1031-1048, 1982.

Bodvarsson, G. S., Pruess, K., Stefansson, V., and E. T. Eliasson, "Modeling Studies of the Natural State of the Krafla Geothermal Field, Iceland," paper presented at the Eighth Annual Workshop on Geothermal Reservoir Engineering, Stanford University, December 14-16. 1982.

Bodvarsson, G. S., Vonder Haar, S., Wilt, M., and Tsang, C. F., "Preliminary Estimation of the Reservoir Capacity and the Longevity of the Baca Geothermal Field, New Mexico," to be published in Water Resources Research, 1983.

Cuellar, G., "The Ahuachapán Geothermal Field, El Salvador," in Geothermal Systems, Principles and Case Histories, L. Rybach and L. J. P. Muffler (Editors), John Wiley and Sons, Ltd., 1981.

Giovannoni, A., Allegrini, G., Cappetti, G., and Celati, R., "First Results of a Reinjection Experiment at Larderello," Proc. Seventh Workshop on Geothermal Reservoir Engineering, Stanford, December 1981, SGP-TR-55.

Grant, M. A., "Permeability Reduction Factors at Wairakei," paper 77-HT-52, presented at AIChE-ASME Heat Transfer Conference, Salt Lake City, Utah, August 1977.

Horne, R., "Geothermal Reinjection Experience in Japan," paper SPE-9925, presented at the California Regional SPE Meeting, Bakersfield, California, March 1981.

International Formulation Committee, "A Formulation of the Thermodynamic Properties of Ordinary Water Substance," IFC Secretariat, Dusseldorf, Germany, 1967.

Jonsson, V. K., "Two-Dimensional Simulation of Cold Water Injection into a Two-Phase Geothermal Reservoir," Lawrence Berkeley Laboratory, unpublished report, August 1979.

Kasameyer, P., and R. Schroeder, "Thermal Depletion of Liquid-Dominated Geothermal Reservoirs with Fracture and Pore Permeability," UCRL-77323, preprint, 1975.

Lai, H. S., Bodvarsson, G. S., and Pruess, K., "Verification of the MINC Method," Lawrence Berkeley Laboratory, paper in preparation, 1983.

Lippmann, M. J., Tsang, C. F., and P. A. Witherspoon, "Analysis of the Response of Geothermal Reservoirs under Injection and Production Procedures," paper SPE-6537, presented at the 47th Annual California Regional Meeting of the SPE, Bakersfield, California, 1977.

Morris, C. M., and Campbell, D. A., "Geothermal Reservoir Energy Recovery: A Three-Dimensional Simulation Study of the East Mesa Field," paper SPE-8229, presented at the 54th Annual Fall Technical Conference and Exhibition of the SPE, Las Vegas, September 1979.

O'Sullivan, M. J., "A Similarity Method for Geothermal Well Test Analysis," Water Resources Research, Vol. 17, p. 390-398, 1981.

O'Sullivan, M. J., and K. Pruess, "Numerical Studies of the Energy Sweep in Five-Spot Geothermal Production/Injection Systems," Proc. 6th Workshop on Geothermal Reservoir Engineering, Stanford University, p. 204-212, 1980.

Pruess, K., "Heat Transfer in Fractured Geothermal Reservoirs with Boiling," Water Resources Research, in press, 1983a.

Pruess, K., "Development of the General Purpose Simulator MULKOM," Lawrence Berkeley Laboratory, Earth Sciences Division, Annual Report 1982, Berkeley, California, 1983b.

Pruess, K., and Karasaki, K., "Proximity Functions for Modeling Fluid and Heat Flow in Reservoirs with Stochastic Fracture Distributions," paper presented at the Eighth Annual Workshop on Geothermal Reservoir Engineering, Stanford University, December 1982.

Pruess, K., and Narasimhan, T. N., "A Practical Method for Modeling Fluid and Heat Flow in Fractured Porous Media," Proc. 6th Symp. on Reservoir Simulation (Paper SPE-10509), New Orleans, Louisiana, February 1982.

Pruess, K., Bodvarsson, G. S., Stefansson, V., and E. T. Eliasson, "A Quasi-Three-Dimensional Model of Well Performance at the Krafla Geothermal Field, Iceland," in preparation, 1983.

Pruess, K., and Schroeder, R. C., "SHAFT79 User's Manual," Lawrence Berkeley Laboratory Report LBL-10861, Berkeley, California, March 1980.

Schroeder, R. C., O'Sullivan, M. J., Pruess, K., Celati, R., and Ruffilli, C., "Reinjection Studies of Vapor-Dominated Systems," Geothermics, Vol. 11, No. 2, p. 93-120, 1982.

Stefansson, V., "The Krafla Geothermal Field, Northeast Iceland," in: Geothermal Systems, Principles and Case Histories, L. Rybach and L. J. P. Muffler (Editors), p. 273-294, 1981.

Stefansson, V., Gudmundsson, A., Steingrimsson, B., Armannsson, H., Franzson, H., Sigurdsson, O., and T. Hauksson, "Krafla-Well KJ-13," Report by the Icelandic Energy Authority, OS82046/JHD07, 1982.

Tsang, C. F., Mangold, D., Doughty, C., and Lippmann, M. J., "Prediction of Reinjection Effects in the Cerro Prieto Geothermal System," Proc. 4th Symposium on the Cerro Prieto Geothermal Field, August 1982.

Warren, J. E., and Root, P. J., "The Behavior of Naturally Fractured Reservoirs," Society of Petroleum Engineers Journal, September 1963, pp. 245-255.

Weber, K. J., and M. Bakker, "Fracture and Vuggy Porosity," Paper SPE-10332, presented at the 56th Annual Meeting of the SPE, San Antonio, Texas, October 5-7, 1981.

Witherspoon, P. A., Bodvarsson, G. S., Pruess, K., and C. F. Tsang, "Energy Recovery by Water Injection," LBL-14820, Invited Paper Presented at the Geothermal Resources Council Workshop on Fractures in Geothermal Reservoirs, Honolulu, Hawaii, August 1982.

Table 1. Fixed Parameters

Rock Matrix	
Grain Density	2650 kg/m^3
Specific Heat	1000 J/kg·°C
Thermal Conductivity	2.0 W/m·°C
Porosity	0.05
Permeability	10^{-17} m^2
Reservoir Thickness	1000 m
Fractures	
Average Porosity	0.01
Average Permeability x Thickness	2×10^{-12} m^3
Relative Permeability	
Linear Curves	$S_{\ell r} = .30$
	$S_{sr} = .05$
Initial Conditions	
Temperature	300°C
Well Parameters	
Productivity Index	7.5×10^{-14} m^3
Bottomhole Pressure	2.0 MPa
Injection Enthalpy	6.32×10^5 J/kg
Separator Conditions	
Pressure	0.9 MPa
Temperature	175.4°C

Table 2. Variable Parameters

Production Well Spacing (a)	250, 500, 1000 m
Fracture Spacing	10, 50, 250 m
Initial Vapor Saturation	0.1, 0.3
Injection Factor	0, 0.5, 1.0

(a) The distance between production and injection wells is a factor $1/\sqrt{2} \simeq .71$ smaller.

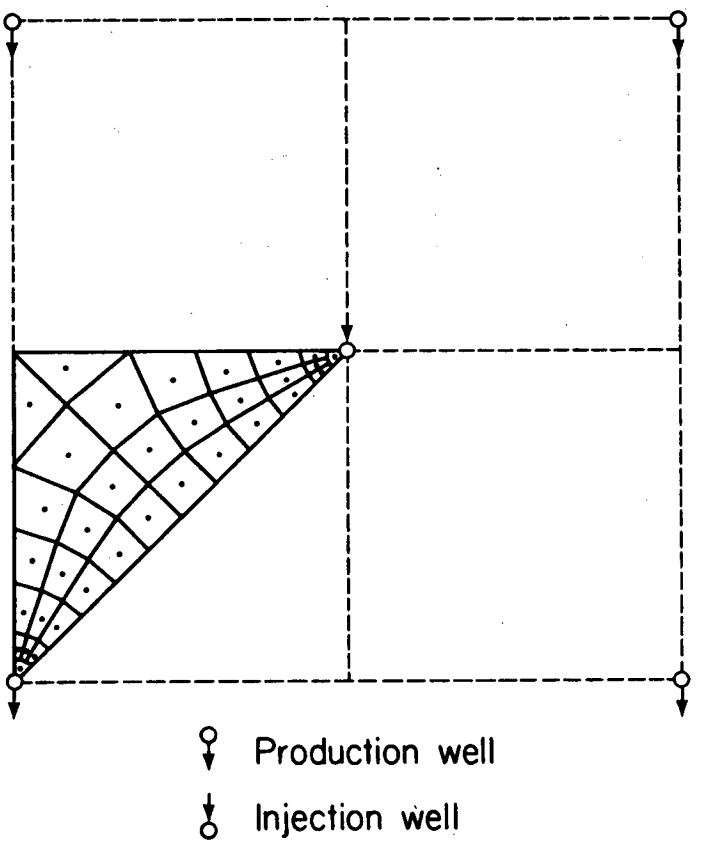

XBL 8010-12543

Figure 1. Porous media mesh for five-spot well pattern.

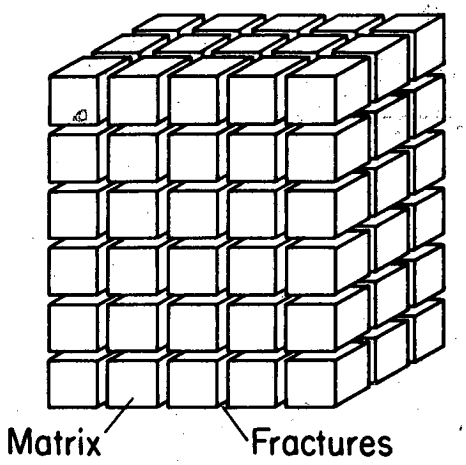

a.

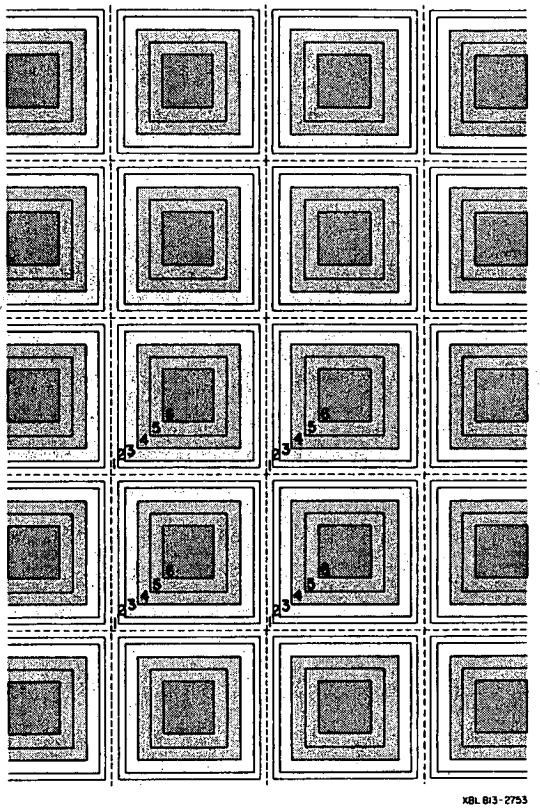

b.

Figure 2. (a) Idealized model of a fractured porous medium; (b) Schematic computational mesh (two-dimensional case).

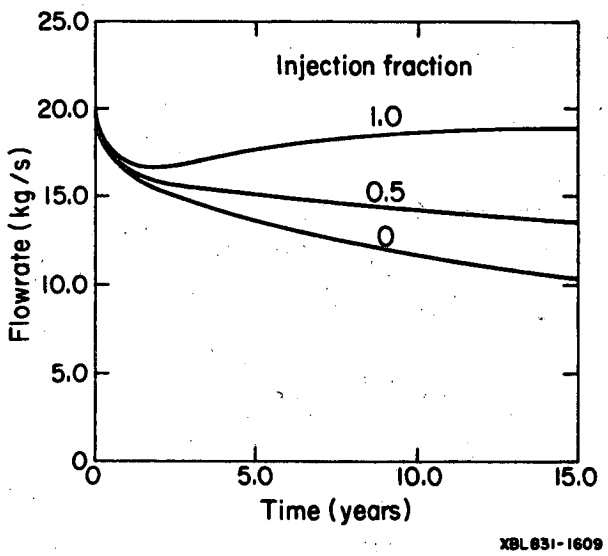

Figure 3. Production rate for 1000 m production well spacing, 250 m fracture spacing, and initial vapor saturation of 10%.

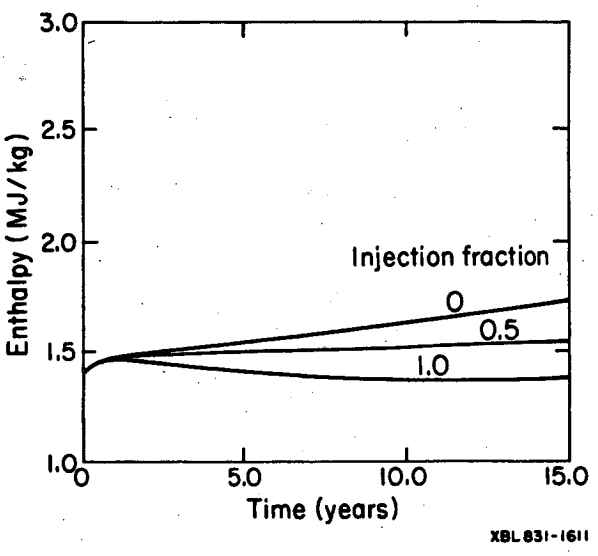

Figure 4. Flowing enthalpy for 1000 m production well spacing, 250 m fracture spacing, and initial vapor saturation of 10%.

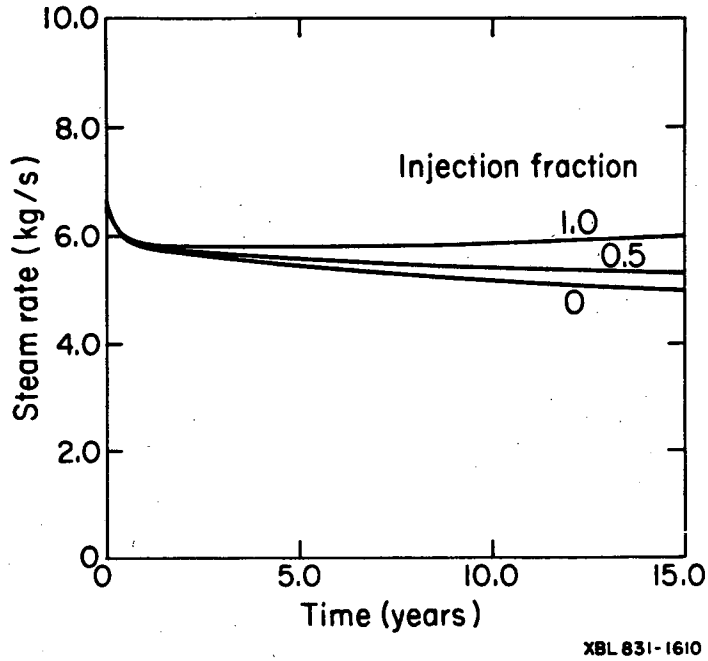

Figure 5. Steam rate at the separators for 1000 m production well spacing, 250 m fracture spacing, and initial vapor saturation of 10%.

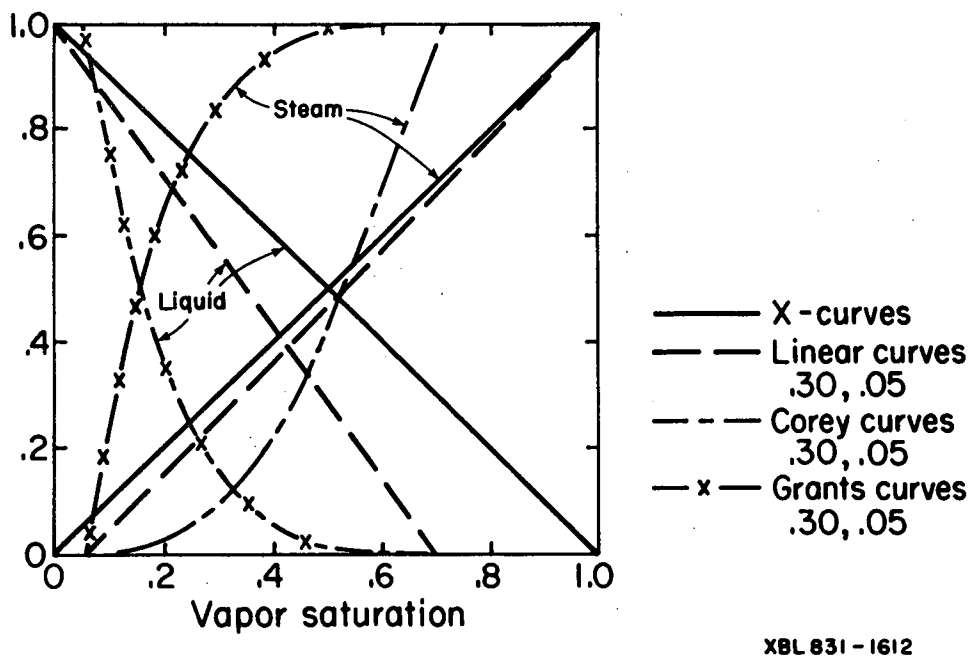

Figure 6. Relative permeability curves used in the analytical study.

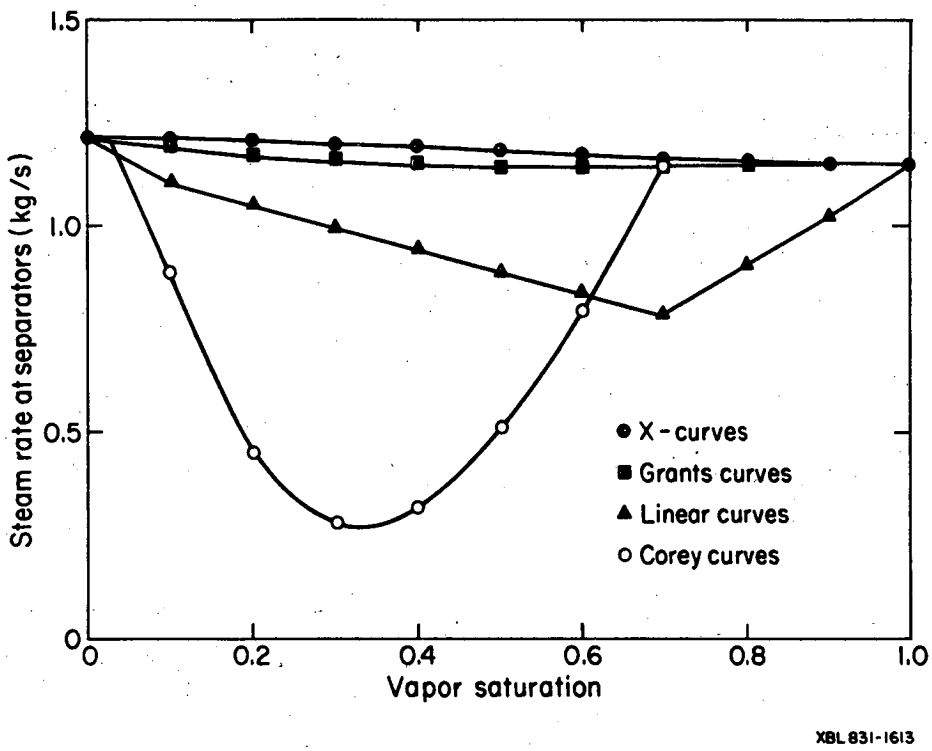

Figure 7. Steam rate at the separators versus vapor saturation for different relative permeability curves.

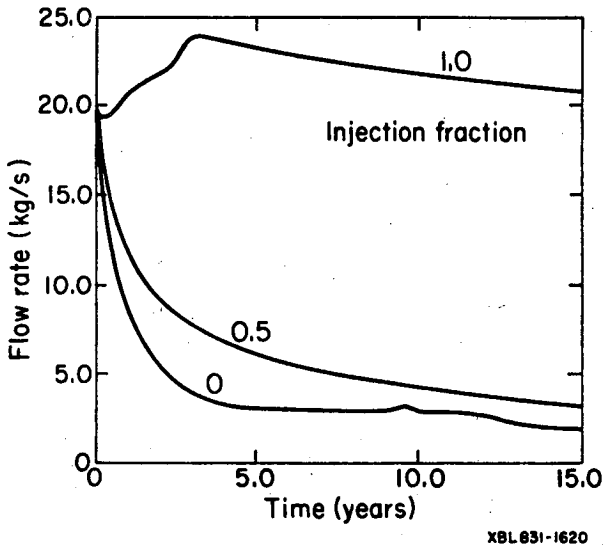

Figure 8. Production rate for 250 m production well spacing, 250 m fracture spacing, and initial vapor saturation of 10%.

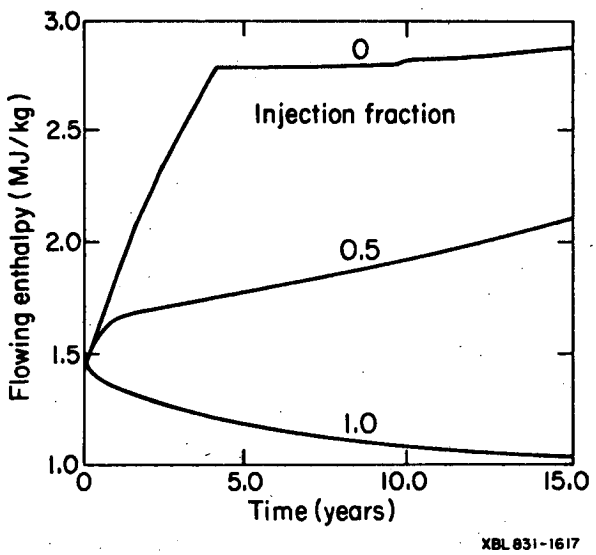

Figure 9. Flowing enthalpy for 250 m production well spacing, 250 m fracture spacing, and initial vapor saturation of 10%.

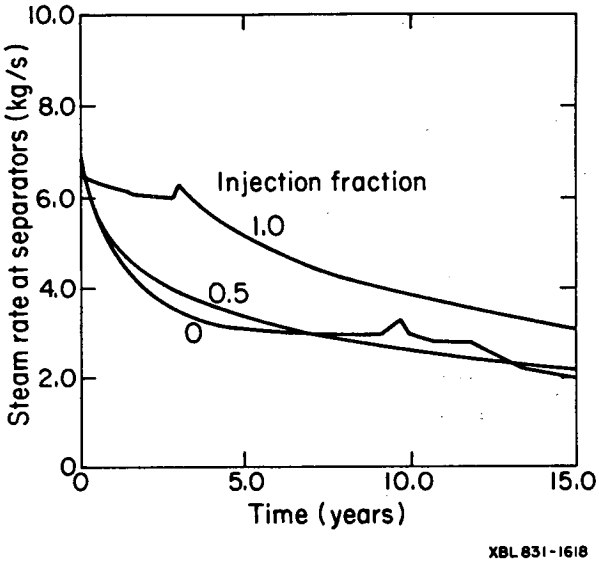

Figure 10. Steam rate at the separators for 250 m production well spacing, 250 m fracture spacing, and initial vapor saturation of 10%.

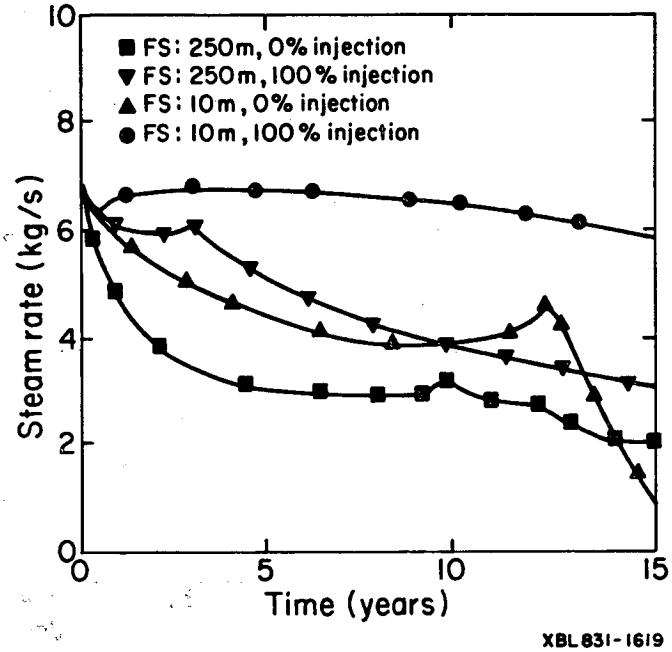

Figure 11. Steam rate at the separators for different fracture spacings and injection fractions. The production well spacing is 250 m.

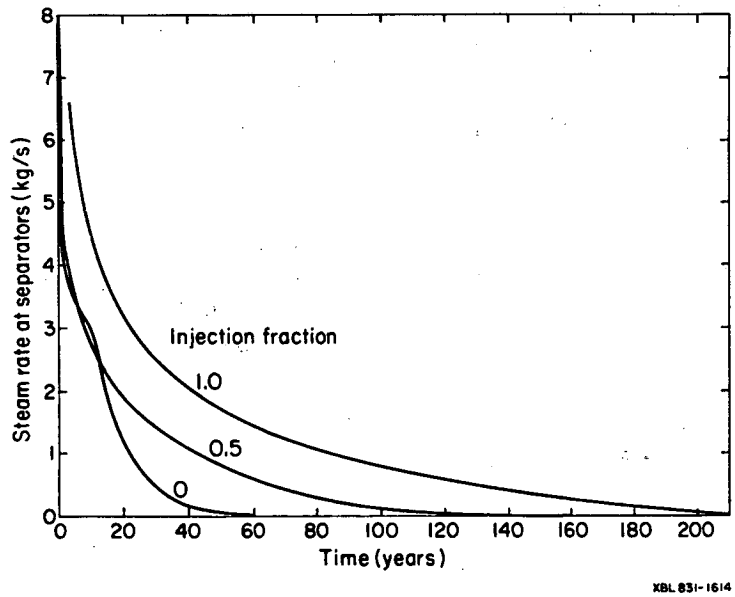

Figure 12. Steam rate at the separators for 250 m production well spacing and 250 m fracture spacing.

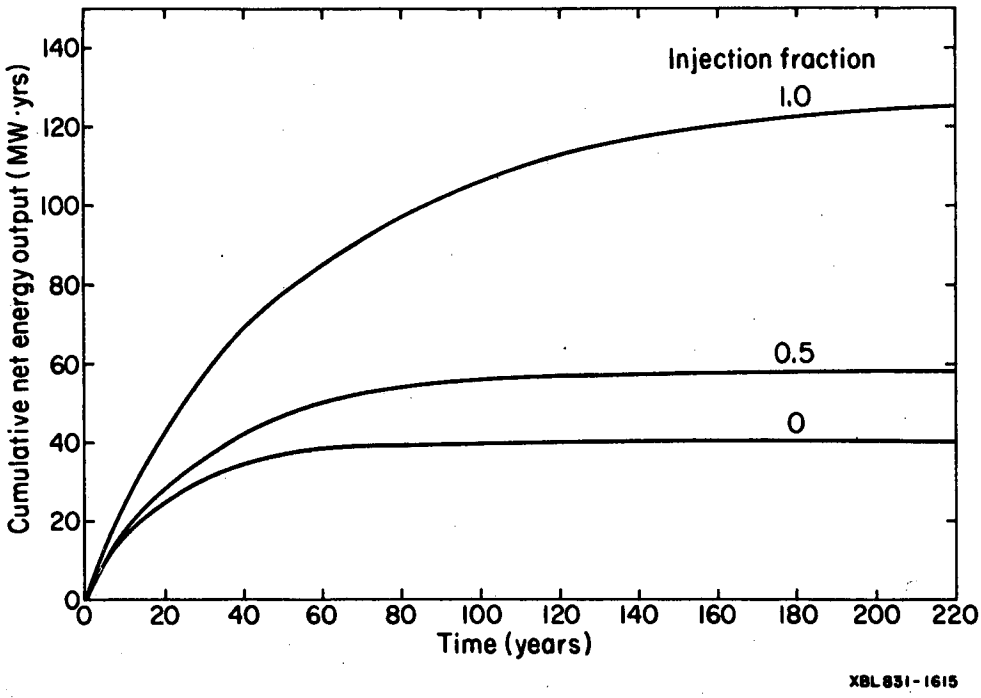

Figure 13. Cumulative net electric energy output for 250 m production well spacing and 250 m fracture spacing.

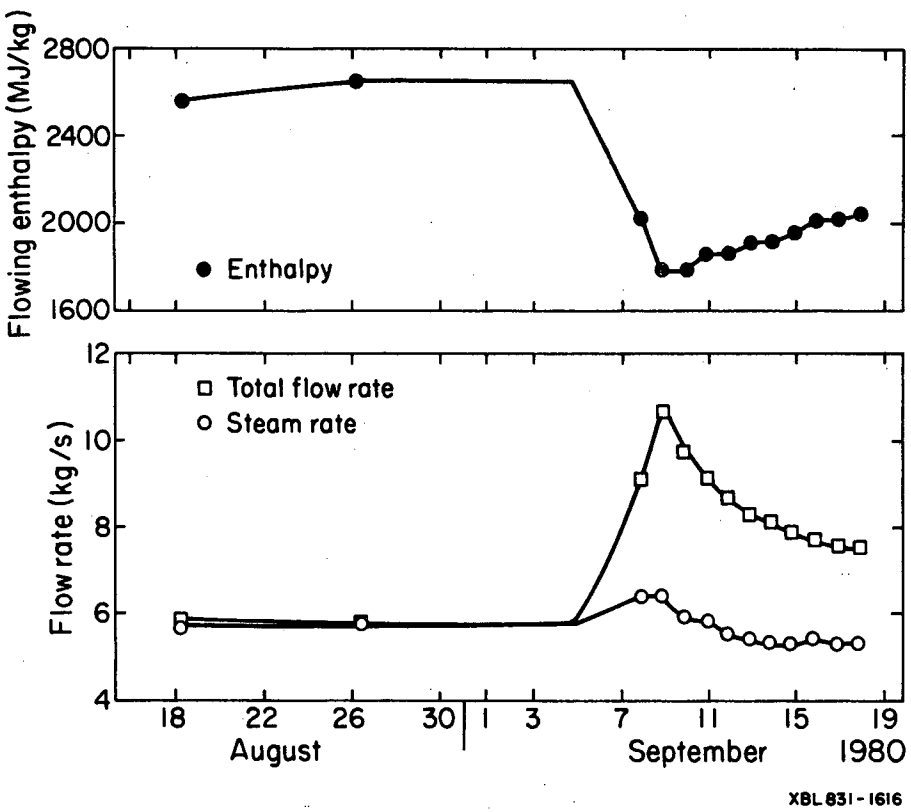

Figure 14. Flow data for well KJ-13 at the Krafla geothermal field (from Stefansson et al., 1982).

TECHNICAL INFORMATION DEPARTMENT
LAWRENCE BERKELEY LABORATORY
UNIVERSITY OF CALIFORNIA
BERKELEY, CALIFORNIA 94720